# Deviation Model-Based Control of Synchronous Reluctance Motor Drives with Reduced Parameter Dependency

*Ehsan Daryabeigi[1], Ahmad Mirzaei[2*], Hossein Abootorabi Zarchi[3], Sadegh Vaez-Zadeh[4]*

[1]Department of Electrical Engineering, Campus of Azadi, Yazd University, Yazd, Iran

[2]Department of Electrical Engineering, Faculty of Engineering, Yazd University, Yazd, Iran

[3]Department of Electrical Engineering, Faculty of Engineering, Ferdowsi University of Mashhad, Mashhad, Iran

[4]Advanced Motion Systems Research Laboratory and Center of Excellence on Applied Electromagnetic Systems, School of Electrical and Computer Engineering, College of Engineering University of Tehran, Tehran, Iran

e.daryabeigi@gmail.com, *mirzaei@yazd.ac.ir, abootorabi@um.ac.ir, vaezs@ut.ac.ir

*Abstract*—**Control issue in electrical drives mainly deals with the dynamic behavior, which is based on the deviation of variables. The deviations play a straightforward role in presenting the various capabilities and merits of the electric drive systems. This paper describes, for the first time, a deviation based torque control (TC) of synchronous reluctance motor (SynRM) drives with no need to know the motor parameters. The proposed control system is designed by using a normalized deviation model to derive linear and simple relationships amongst different machine signals. Therefore, the commonly used PI current regulators are replaced by novel deviation equations. As a result, the proposed approach provides facilities to electric drives, including control system simplicity, parameter independency, and no need for controller tuning. The theoretical findings are verified by those of experiments. The obtained results are reported for a typical SynRM drive. In addition, performance comparison of the control system with a general PI controller-based field oriented control (FOC) scheme is carried out. It is expected that the proposed approach contribute to other electrical drives to simplify the machine equations, reduce control complexities such as the number of conventional controllers, and overcome the problem of machine parameter dependency.**

*Index Terms*— **Deviation model, SynRM, torque control, normalized model.**

## I. INTRODUCTION

The synchronous reluctance motor (SynRM) has received much attention for many applications due to its cold rotor and simple and rugged construction. Also, it is not based on rare-earth magnets. Recently, ABB has commercially developed high output SynRM packages up to 350 kW power ranges [1]. Moreover, a multitude of techniques for control of SynRM drives has been proposed [2-6]. Among them, the direct torque control (DTC) and field-oriented control (FOC) methods were completely developed and today are mature from the industrial point of view. DTC, is widely adopted for ac motor drives due to its fast dynamic characteristics and robust implementation. Unlike FOC, DTC does not require any current regulator and is not very sensible to the parameter detuning [7]. On the other hand, the FOC scheme is characterized by the presence of PI current regulators and coordinate transformations. As a consequence, a straightforward limitation of the current amplitude can be applied.

Variations of machine variables are usually based on a first order-differentiating process, which are finally transferred

to a deviation format [6], [8], [9]. One of the first uses of deviation is related to the basic DTC scheme, where the flux linkage deviation vector is equal to the time deviation multiplied by voltage vector [10]. By differentiating electromagnetic torque equation, and transferring it into a deviation form, a linear relationship is achieved to study torque dynamic behavior [10-14]. In another work, a linear equation is achieved by using deviation of some state variables including stator flux linkage, load angle and quadrature component of stator current [11]. The work proposes a predictive control model-based method extracted from the deviation equations. The effects produced by a given voltage vector on stator flux linkage and torque variations were investigated based on deviation equations for the basic concept of DTC of induction machines in [12]. In [13], by using a differential model based deviation, a combined method was proposed for control of a linear induction motor. Furthermore, an indicator to identify transient state in a SynRM has been proposed based on a deviation equation [3]. In another application, for a sensorless control of permanent magnet synchronous motor at low speed, an algorithm based on current deviations was proposed [14]. In addition, some model free control methods have been proposed based on predictive process [15]. In [15], although a model free predictive current control is proposed to deal with tracking current references, torque or speed control is not discussed there. A Predictive-Based Hybrid direct torque control has been recently proposed to drive IPMSM motors as a fast and simple method [16]. In the reference, despite conventional deviation equations is used to achieve a control low, load angle deviation reference is calculated by a dynamic equation based on parameters. Albeit various advanced control methods have been proposed to deal with challenges of the traditional controllers in torque control mode, using such methods could generally have some complexities because of parameter dependencies and high computational burden [17].

Despite some reported works about using deviation operator [9-14], there are few references which present a comprehensive study on potential of deviation modelling for electrical drives control [18], [19]. Model-based direct flux vector control of permanent magnet synchronous motor drives in [18], [19] calculates the direct axis reference voltage by using a load angle variation. However, the proposed controller is very sensitive to the parameter detuning. Meanwhile, normalization procedures could recently capture interests to deal with some complexities and parameter dependencies for resonant converters [20].

Implying normalization concept and deviation model can provide facilities to overcome the mentioned drawbacks. This matter is developed for electric drive application for the first time in this work. So that, the aim of this paper is to present a deviation model-based TC of SynRM drives with no need of knowledge of the motor parameters. In order to simplicity, a SynRM drive is chosen as an example in this research work. However, the results can be developed for other electrical machine drives. Hence, a deviation based torque control (DevC) of synchronous reluctance motor drives is presented. The closed-loop controlled variables are the deviation of two-axis stator current components in the rotor reference frame. These two are combined to obtain the torque control. Therefore, the proposed control scheme combines the features of the DTC with the ones of current vector controller: simplicity, robustness, and current control.

So far, two proportional–integral (PI) regulators have been conventionally used for the flux and torque control loops of SynRM drives. This paper provides a version of current vector control where PI regulators are replaced by two novel deviation equations. As a result, there is no need for PI calibration, and the dynamic response of closed-loop control is matched up with those of the machine invariant with the torque and speed operating point (whereas PI regulators would require gain adaptation throughout the torque-speed domain) [21].

This paper is organized as follows. In section II, after presentation of SynRM equations, deviation operator and deviation model of SynRM are described respectively. Then, the proposed deviation model is further developed toward a normalized model. In section III, deviation model-based DTC of SynRM drives is described. In section IV, The theoretical findings are verified by simulation and experimental tests. Eventually, a conclusion of the results is presented.

## II. DEVIATION MODEL OF SYNRM

The SynRM $d$–$q$ axis equations in the rotor reference frame, is given by [3]:

$$V_d = R_s.i_d + \frac{d\lambda_d}{dt} - \omega_e \lambda_q ,$$
(1)

$$V_q = R_s.i_q + \frac{d\lambda_q}{dt} + \omega_e \lambda_d .$$
(2)

With:

$$\lambda_q = L_q i_q ,$$
(3)

$$\lambda_d = L_d i_d ,$$
(4)

$$\lambda_s = \sqrt{\lambda_q^2 + \lambda_d^2} ,$$
(5)

$$i_d = \frac{\sqrt{\lambda_s^2 - \lambda_q^2}}{L_d} ,$$
(6)

where $\lambda_d$ and $\lambda_q$ are components of stator flux linkage magnitude '$\lambda_s$', $v_d$ and $v_q$ are stator voltages, $i_d$ and $i_q$ are stator currents, $L_d$ and $L_q$ are stator inductances, which are all in $d$- and $q$-axis rotor reference frame. In addition, the inductance variations caused by saturation effects are considered by a lookup table based on experimental magnetization data [2]. $R_s$ is stator resistance, and $\omega_e$ is the rotor electrical angular velocity. The developed reluctance torque is [3]:

$$T_e = \frac{3P}{2}(\lambda_d i_q - \lambda_q i_d) = \frac{3P}{2}(L_d - L_q)i_q i_d ,$$
(7)

where $P$ is the number of pole pairs.

A deviation transfer can be generally achieved either directly by a differential equation or indirectly by differentiating an equation such as (8). After that, the equation is linearized and the differential operator is changed to a deviation operator "$\Delta$", as follows:

$$z = f(x,y) \xrightarrow{\phantom{aa}d\phantom{aa}} dz = F(x,dx,y,dy) \xrightarrow{\phantom{aa}d \to \Delta\phantom{aa}} \Delta z = F(x, \Delta x, y, \Delta y), \tag{8}$$

where "$x$", "$y$", and "$z$" are typical independent and dependent variables, respectively. Also, "$f$" and "$F$" are typical functions based on the variables. Here, "$\Delta$", as deviation operator, denotes a small deviation of the respective variable from the operation point. In spite of some similarities between deviation modeling and small signal method, a deviation model can comprise terms of both small-scale and large-scale signals with together, while small signal modeling just includes those of small-scale.
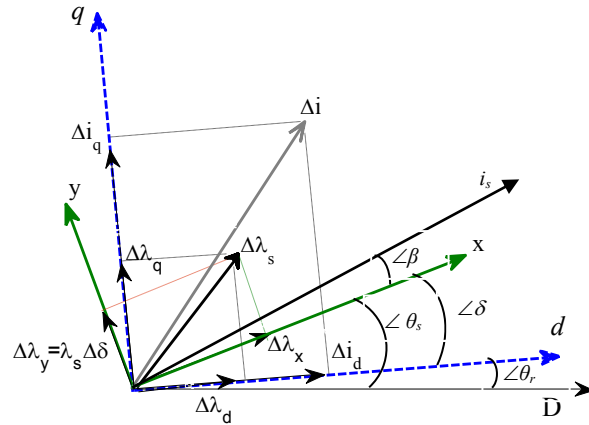


Fig. 1. Vector diagram of SynRM motor including dynamic movements, where $x$-$y$ axis, $d$-$q$ axis, and $D$-$Q$ axis represent stator flux, rotor, and stationary reference frames, respectively.

A deviation vector diagram of the flux linkage and stator current can be found in Fig. 1. Torque deviation can be achieved by applying deviation transfer (8) to the torque equation, (7), using stator current component deviations, as follows:

$$\frac{\Delta T_e}{T_e} = \frac{\Delta i_q}{i_q} + \frac{\Delta i_d}{i_d}. \tag{9}$$

On the other hand, a normalized version of the deviation equation (9) is given with respect to mean values, as:

$$\frac{\Delta T_e}{\hat{T}_e} = \frac{\Delta i_q}{\hat{i}_q} + \frac{\Delta i_d}{\hat{i}_d} \Rightarrow \Delta T_{en} = \Delta i_{qn} + \Delta i_{dn}, \tag{10}$$

where all variables with a superscript "$\wedge$" are mean values. Equation (10) means that the normalized torque ripple '$\Delta T_{en}$' is the sum of those of the current components '$\Delta i_{qn}$' and '$\Delta i_{dn}$' at any operating point in the rotor reference frame. For more details, refer to the Appendix. Furthermore, normalized flux linkage deviation can be given as:

$$\Delta \lambda_n = \cos^2 \delta \Delta i_{dn} + \sin^2 \delta \Delta i_{qn} \tag{11}$$

It is known that the steady state values of machine variables are disturbed under transient state. Therefore, transient voltage terms would be significantly vital in control process. Since, the transient relationships based on the deviation currents can be given as:

$$V_d^t = \frac{\lambda_s \cos \delta}{T_s} \Delta i_{dn},$$
(12)

$$V_q^t = \frac{\lambda_s \sin \delta}{T_s} \Delta i_{qn},$$
(13)

where $V_d^t$, $V_q^t$ and $T_s$ are transient terms of the $d$-$q$ axis voltages (1-2) and sampling time, respectively. It means that the normalized deviation of currents can notably undergo changes by the voltages. Since the sign of flux linkage and torque/load angle are respectively positive and as same as those of torque, the transient voltage proportionalities can be given as:

$$V_d^t \propto \Delta i_{dn},$$
(14)

$$V_q^t \propto sign(T_e) \Delta i_{qn}.$$
(15)

As a result, the normalized deviation currents can be dynamically controlled by controlling stator voltage.

To achieve a deviation signal in discrete-time representation of a system, a general way can be proposed as follows:

$$\Delta Z_n = 2 \frac{Z(k) - Z(k-1)}{Z(k) + Z(k-1)},$$
(16)

where "$Z$", "$k$", and "$\Delta Z_n$" are an arbitrary signal, sampling number, and normalized version of the signal, respectively. Hence, torque, current and flux-linkage deviations are calculated through (16). In addition the defined maximum value for (16) is 1.

Characteristics of the SynRM motor are given in Table I. The experimental results, using a PC-based prototype system, validate the mathematical findings based on a normalized version of the deviation equations. For instance, Fig. 2 confirms that the torque deviation is equal to the sum of $d$ and $q$-axis current deviations in a normalized form (10). As an advantage, the achieved relationships (10)-(13) not only are independent of the machine parameters but also include variation of state variables, which help have a more accurate view on dynamic behavior.

TABLE1. SPECIFICATIONS OF THREE-PHASE SYNRM FOR SIMULATION AND EXPERIMENT.

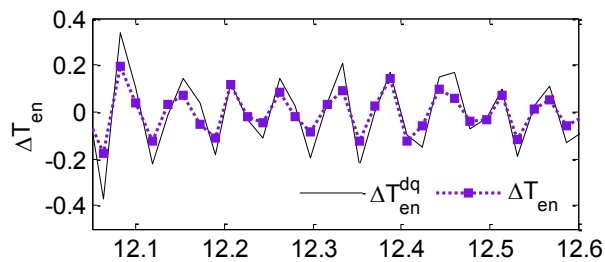| | | |
|---|---|---|
| $P_n = 370\,W$ | $V_n = 230\,V$ | $I_n = 2.8\,A$ |
| $L_{md,un\,Sat} = 232\;mH$ | $L_{md,\,Sat} = 178\,mH$ | $L_{mq} = 118\,mH$ |
| $R_s = 2.95\,\Omega$ | $f_n = 60$ Hz | $No.\ of\ Poles = 4$ |
| $T_{en} = 1.9\,Nm$ | $J_m = .015\,Kg.m^2$ | $B_m = .003$ Nm/rad/sec |

Fig. 2. Experimental results for torque deviation by using (10), depicted over time(s).

The proposed approach presents a simplified model of SynRMs, which can be easily developed for others. Considering the mathematical results, the deviation model is a simple approach to deal with some challenges of machines dynamic behavior analyses. As an application of the modeling, a control system will be developed in the next section.

III. DEVIATION MODEL-BASED DTC OF SYNRM DRIVES

In a standard field-oriented control method, the reference currents are generated to control the machine torque/speed and flux in the stator flux or rotor reference frame. In this regard, the torque and flux are controlled either indirectly by closed-loop controllers or directly by using dynamic relationships. Each of them has their own challenges including the time delay and tuning of controllers, and the dependency on parameter variations, respectively. Therefore, a proper control method should avoid complexities attributed to the controllers and parameter dependency as far as possible [21, 22]. To follow these suggestions, the deviation model is studied to explore a proper control method for SynRM drives in the rotor reference frame. In this regard torque and flux linkage deviations (10) and (11) are used to transfer torque and flux linkage control to current control as follows:

$$\Delta i_{qn}^* = \frac{T_e^* - T_e(k)}{T_e^*(k)} - \Delta i_{dn}^* , \qquad (17)$$

$$\Delta i_{dn}^* = (\tan^2 \delta + 1)\Delta \lambda_{sn}^* - \tan^2 \delta \Delta i_{qn}^* , \qquad (18)$$

where

$$\Delta \lambda_{sn}^* = \frac{\lambda_s^* - \lambda_s(k)}{\lambda_s^*} , \qquad (19)$$

whereas, a star " * " denotes a reference value. Using (17)-(19), a deviation current control system is proposed as in Fig. 3(a). The proposed control system, unlike the standard FOC as illustrated in Fig. 3(b), controls torque and flux linkage just by knowing load angle and without either conventional PI controllers or parameter-dependent equations. Providing flux linkage control and decupling feature between $dq$-axes, FOC employs (6) and decupling terms (1-2) [23], respectively. According to (14)-(15), the reference current deviations are used to determine proper voltage vectors. In this method like FOC, both components of current deviation are transferred from the rotor reference frame to the

stationary reference frame to generate switching pulses by using hysteresis controllers. The proposed control system enjoys a torque control based on the deviation model, which does not suffer from any controller tuning and dependency on parameter variations. Where standard FOC in the rotor reference frame has some difficulties to deal with total flux linkage control, the proposed method easily handles the flux linkage control as will be investigated in the next section.

In addition, supporting wide range of speed regions, an improved estimator is proposed in Fig. 3(c). This estimator is developed as a parallel model including current and voltage models [24]. The proposed estimator needs only $Lq$ value, which is almost constant during operation. By using the method, not only the least number of parameters are required but also the stator resistance can be estimated. The measured maximum error in the estimator is less than 0.03 *Wb*, under full loading and 200% variation of stator resistance in low speeds, which is acceptable [25].
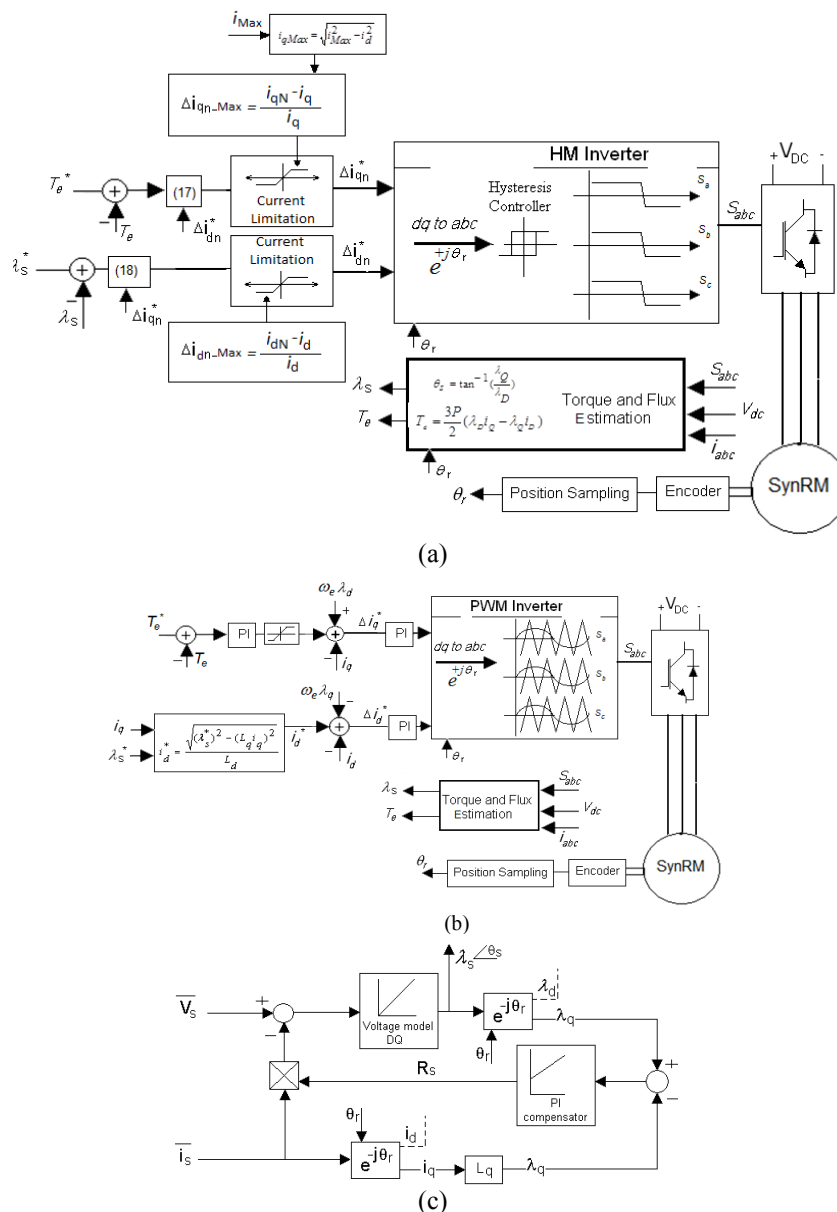


(a)

(b)

(c)

Fig. 3. Structural diagram; a) the proposed control system, and b) standard FOC developed for flux linkage control, c) developed flux estimator.
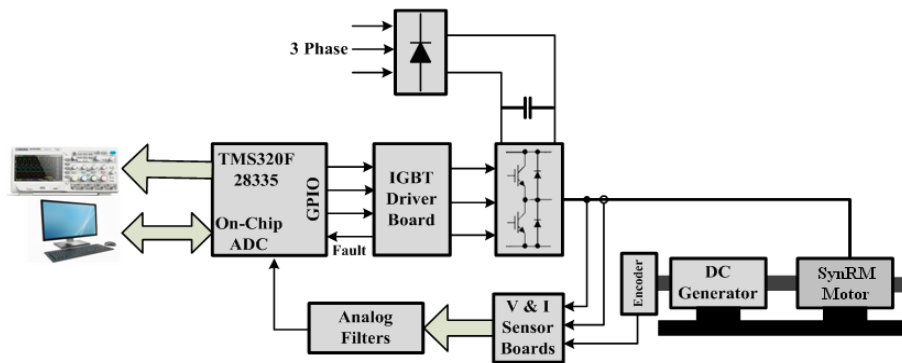
Fig. 4. A block diagram of the prototype setup for experimenal tests.

## IV. RESULTS AND DISCUSSION

To validate the theoretical and mathematical findings of the proposed approach, a SynRM drive with the deviation-model based TC and standard FOC is studied under the same conditions. Both simulation and experimental aspects are investigated. MATLAB software is employed to simulate the system. For experimental evaluation of the proposed system, a DSP-based setup is built and tested. The setup is shown in Fig. 4 and consists of a $370W$ SynRM motor, DC generator as load, voltage source inverter and its driver board, sensor board and a TMS320F28335 discrete signal processor board.
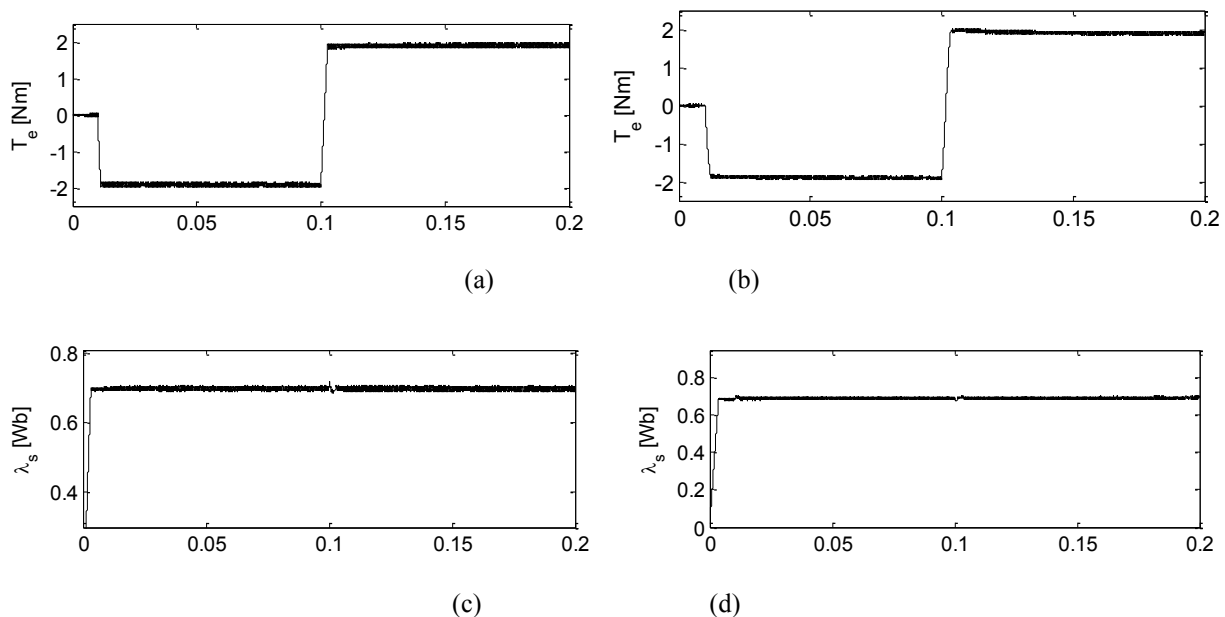


Fig. 5. Simulation results under torque and flux control; *a&b*) generated torque by using DevC and FOC respectively, *c&d*) flux-linkage control by using DevC and FOC respectively, depicted over time(s).

In this section, feasibility and performance quality are studied under steady and transient states. Torque commands of -1.9 Nm and +1.9 Nm are applied at 0.01s and 0.1s, respectively. Torque ripples and control accuracy are evaluated under steady state. On the other hand, dynamic responses are assessed under transient state circumstance. In view of structural comparison, to generate *d-q* axis current deviations, FOC uses three tuned PI closed-loop controllers for

torque and $d$-$q$ axis current components, and an open-loop flux controller based on (6), but the proposed method is just based on two novel deviation type equations (17) and (18). In other cases including inverter structure, DevC enjoys hysteresis controllers, whereas FOC is synchronized to a voltage-controlled PWM with a constant switching frequency 10 *KHz*, as shown in Fig. 3(b). In addition, to have a fair adjustment, FOC uses optimized PI controllers. All the controllers in this work are designed according to a reliable optimization method [26]. The pair coefficients of the PI controller (proportional and integral ones) are "30, 50" and "13.56, 200.8" for current and torque PI controllers, respectively.

*A. Simulation*

The simulation results are shown in Fig. 5 in torque and flux control mode. For the steady state study, a time duration from 0.1s to 0.2s is selected, where torque reference is +1.9 Nm and flux-linkage command is 0.7 *Wb*. The steady state results are shown in Figs. 6(a) and (b) for the proposed deviation based TC (DevC) and FOC, respectively. The steady state study would be done for evaluating torque ripples, which is known as one of the main features of an electrical drive. The presence of ripples can be calculated as [27]:

$$\%\Delta T_{Ave} = 100 \sqrt{\frac{1}{N} \sum_{i=1}^{N} (T_e(i) - T_{Ave})^2} \,, \tag{20}$$

where $N$ and $T_{Ave}$ are the number of samples and the torque average, respectively. The average value of torque is 1.9$Nm$, and its ripple percentage is 1.7% and 1.3% for DevC and FOC, respectively. In addition, the proposed DevC, by using hysteresis controllers, produces an average switching frequency of about 7.5 *KHz*. Although this modulation doesn't provide a constant switching frequency, its average is less than that of FOC with 10 *KHz*.
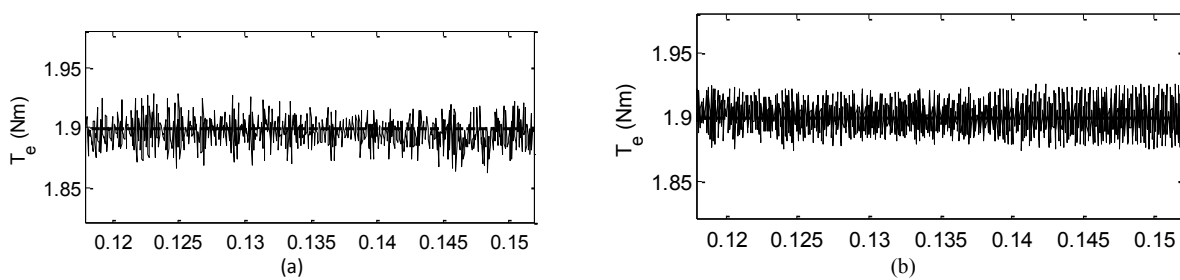


Fig. 6. Simulation results of zoomed torque versus time (s) under FOC and DevC, respectively.

In order to study transient conditions, two intervals are zoomed in Fig. 7, where the torque references, -1.9$Nm$ and +1.9$Nm$, are applied at 0.01$s$ and 0.1$s$, respectively. The results of DevC and FOC are simultaneously shown in Fig. 7. Although, both methods show a high performance in the transient state, DevC scheme presents about 28% faster dynamic compared with that of FOC. In fact, DevC method has a torque response about 2.5 *ms* while the response of FOC is 3.5 *ms*, as shown in Fig. 7(a). As shown in Fig. 7(b), the proposed method meets the torque command in terms of fast dynamic, zero over/under-shoot, and zero steady state error. This matter for FOC shows an overshoot on torque

control. Not only DevC shows a superiority over FOC in terms of dynamic responses, accuracy and simplicity, but also establishes decoupling between flux and torque control, in particular at transient states, as shown in Fig. 7(c). This decoupling feature could be attributed to contribution of $q$-axis and d-axis currents in (18) and (17), respectively, where natural coupling characteristic of the machine is considered as both embedded control terms in deviation control structure. To have a more fair adjustment, decoupling terms are considered in the FOC [23]. Albeit these terms are used to facilitate a suitable decoupling between $d$ and $q$ axis current components in FOC, due to notable coupling between linkage flux and torque producing component (5), these terms can hardly expose a proper decoupling feature between linkage flux and torque producing component. Hence, equation (6) is additionally employed to satisfy this decoupling, as shown in Fig. 3. Nevertheless, as shown in Fig.7(c), whereas FOC is passing the transient coupling state at 1.3$ms$ and with a 3.5% undershoot, DevC dose it at half of the time and with just a 2% overshoot, which is negligible. Although both DevC and FOC could be comparable in decoupling features, DevC could handle this matter without considering parameters and with minimum complexity.
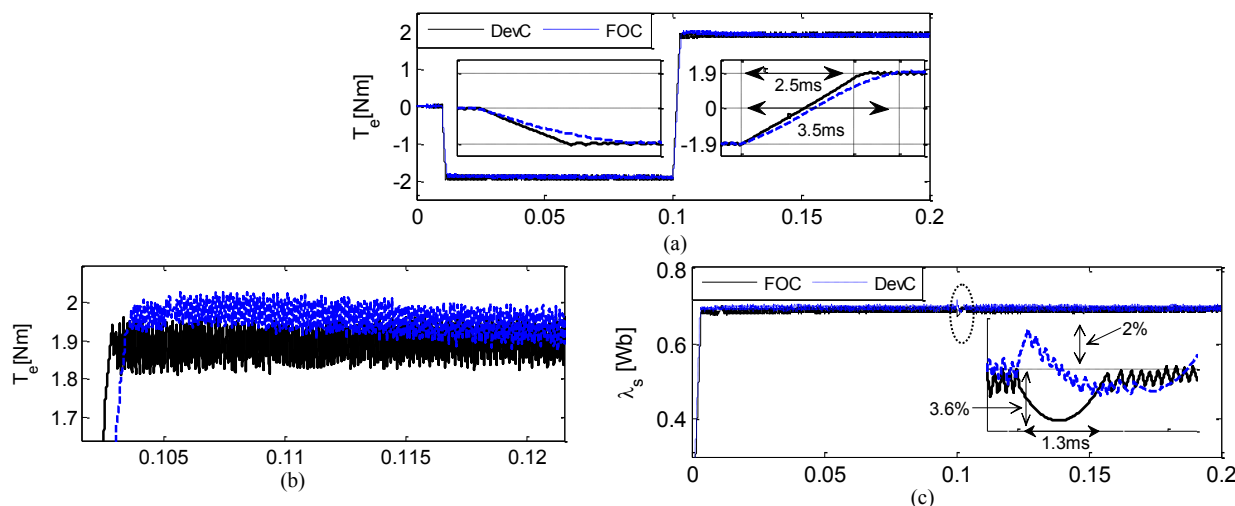


Fig. 7. The transient results under torque control based on DevC and FOC respectively; a) developed torque, b) zoomed torque, and c) flux linkage, depicted over time (s).

*Note*, because of the complexities attributed to FOC method in rotor frame reference, for flux linkage control, generally $d$-axis component control is preferred [23]. Fig. 7(c) shows a phase difference between flux linkage responses of FOC and DevC in facing with the torque commands, while FOC is waiting for control feedbacks caused by $q$-axis current controller to have a reaction, DevC enjoys a control feedback by direct contributing torque reference (17-18), which results in a better damping of coupling effects on the flux control. In addition, FOC with PI feedbacks has some delays, which might cause weaker performances. In order to study robustness of the proposed method against parameter variations under low speed conditions, stator resistance variation is considered for both DevC and FOC under the same conditions. The partial and full loading conditions for step torque commands are equal to 1$Nm$ and 1.9$Nm$ at *0s* and 0.05$s$, respectively, flux linkage is kept constant at 0.7$Wb$, and low speed caused by a loading proportional to speed such as fan load. While torque and flux step commands are being tracked by both methods, the resistance is suddenly

changed at 0.1*s*. Although a maximum range of the stator resistance variation caused by temperature rise and skin effects is reported to be less than 200% [25], a larger variation might be imposed even up to 800% by external factors such as damaged breakers or connections. Here, a maximum variation of 800% on the resistance is considered to evaluate the robustness.
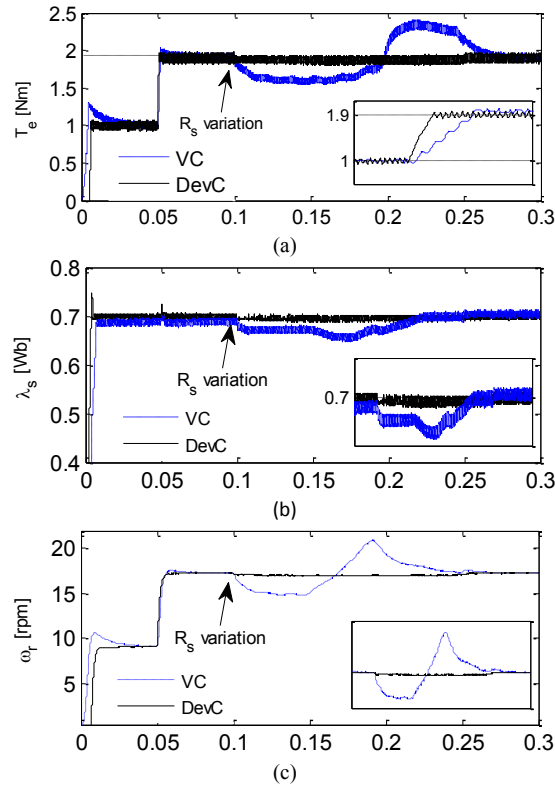


Fig. 8. Simulation results of the stator flux linkage variation test; a) electromagnetic torque, b) flux-linkage, c) Rotor speed, depicted over time(s).

The achieved results are presented in Fig. 8. Although the decupling feature could be significantly improved by considering the terms when applying torque step command at t=0.05*s*, dynamic responses are still weak in comparison with those of DevC for both toque and flux as given in Figs. 8(a&b), respectively. In addition, parameter dependency attributed to FOC controllers exposes destructive effects on both torque and speed variables when a sudden harsh change is imposed on the stator resistance, as seen in Fig.8(b&c). FOC is faced with a fluctuation in torque and speed, as given in Figs. 8(a&c), although temporarily. As it is seen well, DevC perfectly handles this challenge, while FOC is failed to capture the imagination. It means that DevC has succeeded to keep its control ability during the test.

### B. Experimental

The practical results are achieved to verify the achievements of the simulation, considering the same conditions for both experimental and simulation. In this way, the proposed method is assayed in a pragmatic condition with a sampling time 20*μs*. The results are shown in Fig. 9, in torque and flux control mode. As it is well seen in Fig. 9(a), torque dynamic for an step torque command from -1.9 *Nm* to +1.9, is about 2.5 *ms*. Zero steady state error of torque and flux control, in Figs. 9(b&c), represents the DevC control accuracy that discussed in connection with the simulation results.

In addition, switching frequency and torque ripples of less than 2% and 7 kHz are obtained, which confirm those of simulation.

In addition, torque and flux are exactly tracked as expected for a DTC classic method in terms of fast dynamic without under/over shoots. Furthermore, an additional test is done to verify effects of flux control on torque control loop. A constant torque and a step flux linkage commands are applied to the DevC to drive SynRM in experimental conditions. As it is shown in Figs. 10(a) and (b), while flux linkage is tracking its step command at t=0.2s, torque is kept constant at its command. As discussed above, the experimental results support those of theoretical and simulation.
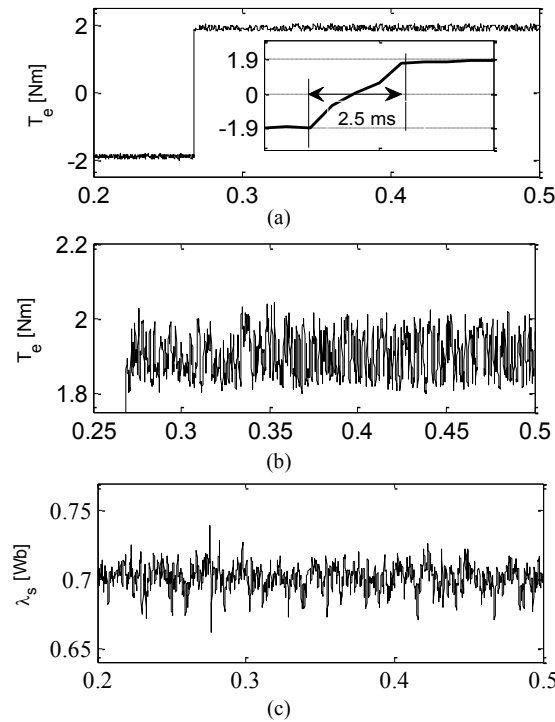


Fig. 9. The results under torque control based on DevC; a) developed torque, b) zoomed torque, c) flux linkage, depicted over time(s).
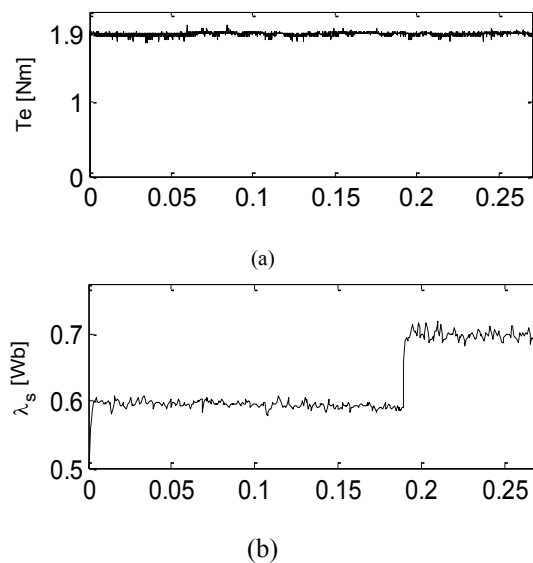


Fig. 10. The transient and steady state results under torque control based on DevC; a) developed torque, b) flux linkage, depicted over time(s).
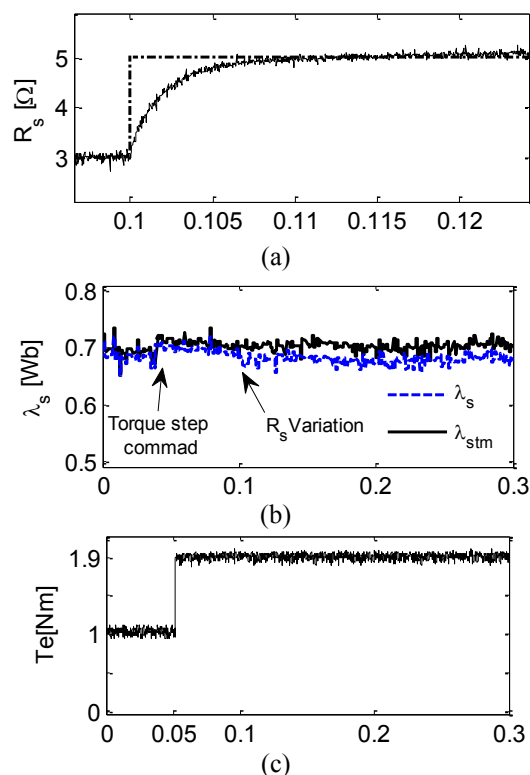
Fig. 11. Experimental results achieved by DevC matched with the developed estimator under stator resistance estimation; a) stator resistance estimation, b) flux linkages, c) torque.

To address the robustness of the proposed drive, an external resistance about 170% $R_s$ is added to the each machine stator phase terminal by a command circuit after voltage sensors. The motor is started by DevC at a torque 1$Nm$, with flux linkage of 0.7 $Wb$, and nominal stator resistance. A step torque command +1.9 $Nm$ is applied at 0.05$s$, when flux linkage is being kept constant at 0.7 $Wb$. After that, external resistances are serially added to the stator windings at 0.1$s$. As illustrated in Fig. 11(a), the estimator is triggered to follow stator resistance variations with a proper dynamic. Subsequently, it improves dynamic response of the flux estimation to deal with the variation as given in Fig. 11(b), which rides of those defects might be reflected on torque control during the sudden variations as represented in Fig. 11(c) [28]. As shown in Fig. 11(b), after resistance variation, there is a small difference about 0.01$Wb$ between estimated flux linkage '$\lambda_{stm}$' and that of calculated by measured magnetization data '$\lambda_s$' [2]. This negligible difference can arise from using a constant $q$-axis inductance in the proposed estimator. As a result, although DevC, as a free-parameter method, doesn't include either control parameters or those of the motor, it should handle motor performance variation caused by the parameters. Hence, these tests could effectively show robustness of the DevC against the parameter variations.

The proposed DevC addresses many of the drawbacks attributed by FOC in comparison with DTC, such as complexity, low robustness, and moderate dynamic responses. As an attractive feature, the proposed method is easily implemented and the experimental results are achieved at the first run of the system, without any need of controller tuning or even specific parameter knowledge in the control procedure.

## V.   CONCLUSION

In this paper, a deviation model was developed for torque control (TC) of SynRM drives. It was found that a normalized version of the model not only makes the dynamic relationships very simple, but also provides parameter independency in the control system. As a result, the proposed deviation model is able to present a simple view of the system dynamic behavior. As an application, the deviation model can be contributed to extract some control methods, as it was applied for the Deviation based TC (DevC) method to drive a SynRM motor in this paper. The proposed approach presented an excellent dynamic behavior both in transient and steady state conditions. In comparison with FOC, DevC facilities flux and torque control, so that it enjoys deviation equations without need of conventional controllers in structure as well as knowledge of the motor parameters, a faster dynamic without under/over shoots, same constant switching frequency and similar torque ripple in performance. As a result, the deviation model in general and the normalized model in particular could open a new window-to analyze and control electrical drives.

*Appendix*

A deviation model of SynRM drives can be calculated based on flux relationships, as follows:

$$\lambda_s = \sqrt{\lambda_q^2 + \lambda_d^2},$$

$$\xrightarrow{d} d\lambda_s = \frac{2\lambda_q d\lambda_q + 2\lambda_d d\lambda_d}{2\sqrt{\lambda_q^2 + \lambda_d^2}} \Rightarrow \Delta\lambda_s = \frac{2\lambda_q \Delta\lambda_q + 2\lambda_d \Delta\lambda_d}{2\sqrt{\lambda_q^2 + \lambda_d^2}} = \sin\delta\Delta\lambda_q + \cos\delta\Delta\lambda_d, \qquad (1A)$$

$$\frac{\Delta\lambda_s}{\lambda_s} = \frac{\lambda_q}{\lambda_s \lambda_q}\sin\delta\Delta\lambda_q + \frac{\lambda_d}{\lambda_s \lambda_d}\cos\delta\Delta\lambda_d \xrightarrow{normalizing} \Delta\lambda_{sn} = (\sin\delta)^2 \Delta\lambda_{qn} + (\cos\delta)^2 \Delta\lambda_{dn}, \qquad (2A)$$

where, $\Delta\lambda_{qn} = \Delta i_{qn}$,   $\Delta\lambda_{dn} = \Delta i_{dn}$, and (2A) is simplified as:

$$\Delta\lambda_{sn} = (\sin\delta)^2 \Delta i_{qn} + (\cos\delta)^2 \Delta i_{dn}. \qquad (3A)$$

In addition, differential and deviation of load angle are respectively presented as:

$$\sin\delta = \frac{\lambda_q}{\sqrt{\lambda_q^2 + \lambda_d^2}} \xrightarrow{d} d\delta = \cos\delta\frac{d\lambda_q}{\lambda_s} - \sin\delta\frac{d\lambda_d}{\lambda_s}$$

$$\xrightarrow{\Delta} \Delta\delta = \cos\delta\frac{\Delta\lambda_q}{\lambda_s} - \sin\delta\frac{\Delta\lambda_d}{\lambda_s} \qquad . \qquad (4A)$$

The deviation is rewritten as:

$$\Delta\delta = \frac{\sin 2\delta}{2}(\Delta i_{qn} - \Delta i_{dn}) \,.$$

(5A)

Furthermore, when orienting the reference frame is considered, y-axis flux deviation, in stator flux oriented frame, could be approximated as

$$\Delta\lambda_y \cong \lambda_s \Delta\delta \,.$$

(6A)

It means if variation of the reference frame position is considered, flux deviation vector includes both *x-y* axis components, as shown in Fig. 1. Otherwise, the deviation vector is just composed of *x*-axis flux deviation that its value is equal to that of total flux deviation.

Also, transient term of the machine voltage equation, in stator flux oriented frame, can be represented in a short interval of $\Delta t = T_S$ as [29]:

$$\vec{V}_S^t T_S \cong \Delta\vec{\lambda}_S = \Delta\lambda_x + j\Delta\lambda_y \,,$$

(7A)

where,

$$\vec{V}_S^t = V_x^t + jV_y^t,$$
$$\Delta\lambda_x = \Delta\lambda_S, \quad \Delta\lambda_y \cong \lambda_S \Delta\delta.$$

(8A)

Equation (7A) is employed to select instantaneous voltage vector in combined control CC [29]. Since, it could be developed to find a relationship between deviation currents and transient voltage vectors. Substituting (3A) and (5A) into (8A), the voltage equation can be achieved as:

$$\begin{bmatrix} V_x^t \\ V_y^t \end{bmatrix} = \frac{\lambda_S}{T_S}\begin{bmatrix} \cos^2\delta & \sin^2\delta \\ -\frac{\sin 2\delta}{2} & \frac{\sin 2\delta}{2} \end{bmatrix}\begin{bmatrix} \Delta i_{dn} \\ \Delta i_{qn} \end{bmatrix}.$$

(9A)

Therefore, the voltage vectors are presented in rotor reference frame as:

$$\begin{bmatrix} V_d^t \\ V_q^t \end{bmatrix} = \frac{\lambda_S}{T_S}\begin{bmatrix} \cos\delta & 0 \\ 0 & \sin\delta \end{bmatrix}\begin{bmatrix} \Delta i_{dn} \\ \Delta i_{qn} \end{bmatrix}.$$

(10A)

It can be easily shown that these voltages are transient parts of the terminal voltages (1-2).

To have a torque deviation based on (7), it can be calculated as:

$$T_e = \frac{3P}{2}(L_d - L_q)i_q i_d \xrightarrow{d} dT_e = \frac{3P}{2}(L_d - L_q)i_q di_d + \frac{3P}{2}(L_d - L_q)i_d di_q . \tag{11A}$$

By dividing both sides of the above equation by (7), it can be achieved as:

$$\frac{dT_e}{T_e} = \frac{\frac{3P}{2}(L_d - L_q)i_q di_d}{\frac{3P}{2}(L_d - L_q)i_q i_d} + \frac{\frac{3P}{2}(L_d - L_q)i_d di_q}{\frac{3P}{2}(L_d - L_q)i_q i_d} = \frac{di_d}{i_d} + \frac{di_q}{i_q} . \tag{12A}$$

Consequently, by using deviation operator, it is rewritten as:

$$\frac{dT_e}{T_e} = \frac{di_d}{i_d} + \frac{di_q}{i_q} \xrightarrow{d \to \Delta} \frac{\Delta T_e}{T_e} = \frac{\Delta i_d}{i_d} + \frac{\Delta i_q}{i_q} , \tag{13A}$$

which is simplified as: $\Delta T_{en} = \Delta i_{qn} + \Delta i_{dn}$.

In order to study stability of the proposed control system, Lyapunov theory is employed. Since the inverter operates in direction of its input signals, it can be concluded that:

$$sign(\Delta i_{sn}) = sign(\Delta i_{sn}^*) . \tag{14A}$$

In addition, if the command current is assumed constant, differential of $\Delta i_{sn}^*$ is given as:

$$d(\Delta i_{sn}^*) = d(\frac{i_s^* - i_s}{i_s^*}) = -\frac{di_s}{i_s^*} . \tag{15A}$$

It can be rewritten in a deviation form as:

$$d(\Delta i_{sn}^*) = -\frac{\Delta i_s}{i_s^*} = -\Delta i_{sn} . \tag{16A}$$

Since (17) and (18) are considered as the heart of the proposed control system, a positive Lyapunov function could be dedicated as:

$$\begin{aligned}
v &= v_1 + v_2 \geq 0 \\
v_1 &= (\Delta T_{en}^* - \Delta i_{dn}^*)^2 \\
v_2 &= ((\tan^2 \delta + 1)\Delta \lambda_{sn}^* - \tan^2 \delta \Delta i_{qn}^*)^2
\end{aligned} . \tag{17A}$$

Since variation of the reference frame position is not considered here, like (3A), the load angle "$\delta$" can be assumed constant. By differentiating (17A) and considering (14A) and (16A),

$$v' = 2(\Delta T_{en}^{*} - \Delta i_{dn}^{*})(-\Delta T_{en} + \Delta i_{dn}) +$$
$$2((\tan^2 \delta + 1)\Delta \lambda_{sn}^{*} - \tan^2 \delta \Delta i_{qn}^{*})(-(\tan^2 \delta + 1)\Delta \lambda_{sn} + \tan^2 \delta \Delta i_{qn}) \quad . \tag{18A}$$

Eq. (18A) is summarized by considering (10), (11) and (16A) as:

$$v' = v_1' + v_2', \tag{19A}$$

where,

$$v_1' = 2\Delta i_{qn}^{*}(-\Delta i_{qn}),$$
$$v_2' = 2\Delta i_{dn}^{*}(-\Delta i_{dn}).$$

According to (14A), (19A) is given as:

$$v' = -2\left|\Delta i_{qn}^{*}\right|\left|\Delta i_{qn}\right| - 2\left|\Delta i_{dn}^{*}\right|\left|\Delta i_{dn}\right| . \tag{20A}$$

Lyapunov stability criterion is considered for an equilibrium point ( $\Delta i_{dn}^{*} = 0$, $\Delta i_{qn}^{*} = 0$) as flows:

$$v_1 = f(\Delta i_{qn}^{*}) = 0 \text{ if and only if} \qquad \Delta i_{qn}^{*} = 0 , \tag{21A}$$

$$v_2 = f(\Delta i_{dn}^{*}) = 0 \text{ if and only if} \qquad \Delta i_{dn}^{*} = 0 , \tag{22A}$$

then,

$$v' < 0 \text{ for all value of } \Delta i_{dn}^{*} \neq 0 , \Delta i_{qn}^{*} \neq 0 \text{ (negative definite)}, \tag{23A}$$

where, $v$ is called a Lyapunov function candidate and the system is stable in the sense of Lyapunov.

## REFERENCES

[1] S. Taghavi and P. Pillay, "A sizing methodology of the SynRM for traction applications," *IEEE Journal of Emerging and Selected Topics in Power Electronic*, vol. 2, no. 2, pp. 329–340, 2014.

[2] H. Abootorabi Zarchi, J. Soltani, and Gh. Arab Markadeh, "Adaptive input–output feedback-linearization-based torque control of synchronous reluctance motor without mechanical sensor," *IEEE Transactions on Industrial Electronics*, vol. 57, no. 1, pp. 375–384, 2010.

[3] E. Daryabeigi, H. Abootorabi Zarchi, G. R. Arab Markadeh, J. Soltani, and F. Blaabjerg, "Online MTPA control approach for synchronous reluctance motor drives based on emotional controller," *IEEE Transactions on Power Electronics*, vol. 30, no. 4, 2015.

[4] H. Abootorabi Zarchi, Gh.R. Arab Markadeh, and J. Soltani, "Direct torque and flux regulation of synchronous reluctance motor drives based on input–output feedback linearization," *Energy Conversion and Management*, vol. 51, no. 1, pp. 71–80, 2010.

[5] H. Abootorabi Zarchi, E. Daryabeigi, Gh. R. Arab Markadeh, and J. Soltani, "Emotional controller (BELBIC)

based DTC for encoderless synchronous reluctance motor drives," *2011 2nd Power Electronics, Drive Systems and Technologies Conference*, 2011, pp. 478 – 483.

[6]  G. H. B. Foo and X. Zhang, "Robust direct torque control of synchronous reluctance motor drives in the field-weakening region," *IEEE Transactions on Power Electronics*, vol. 32, no. 2, pp. 1289–1298, 2017.

[7]  D. Casadei, F. Profumo, G. Serra, and A. Tani, "FOC and DTC: two viable schemes for induction motors torque control," *IEEE Transactions on Power Electronics*, vol. 17, no. 5, pp. 779–787, 2002.

[8]  S. Vaez-Zadeh, *Control of Permanent Magnet Synchronous Motors*. Oxford University Press, 2018.

[9]  B. H. Kenny and R. D. Lorenz, "Stator and rotor flux-based deadbeat direct torque control of induction machines," *IEEE Transactions on Industry Applications*, vol. 39, no. 4, pp. 1093–1101, 2003.

[10]  Y. Cho, K-B. Lee, J-H. Song, and Y. II Lee, "Torque-ripple minimization and fast dynamic scheme for torque predictive control of permanent-magnet synchronous motors," *IEEE Transactions on Power Electronics*, vol. 30, no. 4, pp. 2182-2190, Apr. 2015.

[11]  Y. Ren, Z. Q. Zhu, and J. Liu, "Direct torque control of permanent-magnet synchronous machine drives with a simple duty ratio regulator," *IEEE Transactions on Industrial Electronics,* vol. 61, no.10, 2014.

[12]  D. Casadei, G. Serra, and K. Tani, "Implementation of a direct control algorithm for induction motors based on discrete SVM," *IEEE Transactions on Power Electronics*, vol. 15, no. 4, pp. 769–777, 2000.

[13]  H. Karimi, S. Vaez-Zadeh, and F. Rajaei Salmasi, "Combined vector and direct thrust control of linear induction motors with end effect compensation," *IEEE Transactions on Energy Conversion*, vol. 31, no. 1, pp.196-205, 2016.

[14]  G. Xie, K. Lu, S. Kumar Dwivedi, J. Riber Rosholm, and F. Blaabjerg, "Minimum-voltage vector injection method for sensorless control of PMSM for low-speed operations," *IEEE Transactions on Power Electronics*, vol. 31, no. 2, pp. 1785-1794 Feb. 2016.

[15]  C. K. Lin, J. T. Yu, Y. S. Lai, and H. C. Yu, "Improved model-free predictive current control for synchronous reluctance motor drives," *IEEE Transactions on Industrial Electronics*, vol. 63, no.6, pp.3942-3953, 2016.

[16]  M. J. Navardi, J. Milimonfared, and H. A. Talebi, "Torque and flux ripples minimization of permanent magnet synchronous motor by a predictive-based hybrid direct torque control," *IEEE Journal of Emerging and Selected Topics in Power Electronic*, (early access), 09 May 2018.

[17]  H. Hadla and S. Cruz, "Predictive stator flux and load angle control of synchronous reluctance motor drives operating in a wide speed range," *IEEE Transactions on Industrial Electronics* vol. 64, no. 9, pp. 6950-6959, Sep. 2017.

[18]  G. Pellegrino, B. Boazzo, and Th. M. Jahns, "Plug-in direct-flux vector control of PM synchronous machine drives," *IEEE Transactions on Industry Applications*, vol. 51, no. 5, pp. 3848-3857, 2015.

[19] B. Boazzo and Gi. Pellegrino, "Model-based direct flux vector control of permanent-magnet synchronous motor drives," *IEEE Transactions on Industry Application*, vol. 51, no. 4, pp. 3126-3136, 2015.

[20] S. M. Lucas, Th. C. Naidon, G. G. De Freitas, M. L. da S. Martins, and F. E. Bisogno, "Energy-based normalization for resonant power converters", *IEEE Transaction on Power Electronics*, vol. 33, no. 8, pp. 6526-6536, 2018.

[21] J.W. Finch and D. Giaouris, "Controlled AC electrical drives," *IEEE Transactions on Industrial Electronics*, vol. 55, no. 2, pp. 481-491, 2008.

[22] M. Hinkkanen, H. A. A. Awan, Z. Qu, T. Tuovinen, and F. Briz, "Current control for synchronous motor drives: direct discrete-time pole-placement design," *IEEE Transactions on Industry Application*, vol. 52, no. 2, pp.1530-1541, 2016.

[23] S-C. Agarlita, I. Boldea, and F. Blaabjerg,"High-frequency-injection-assisted active-flux-based sensorless vector control of reluctance synchronous motors, with experiments from zero speed," *IEEE Transactions on Industry Application*, vol. 48, no. 6, pp.1931-1929, Nov. 2012.

[24] I. Boldea, C. Ilie Pitic, C. Lascu, Gh-D. Andreescu, L. Tutelea, F. Blaabjerg, and P. Sandholdt, "DTFC-SVM motion-sensorless control of a PM-assisted reluctance synchronous machine as starter-alternator for hybrid electric vehicles," *IEEE Transactions on Power Electronics,* vol. 21, no. 3, pp-711-719, May 2006.

[25] Zh. Xu and M. Faz Rahman, "Direct torque and flux regulation of an IPM synchronous motor drive using variable structure control approach," *IEEE Transactions on Power Electronics*, vol. 22, no. 6, pp.2487-2498, 2007.

[26] E. Daryabeigi and B. Mirzaeian Dehkordi, "Smart bacterial foraging algorithm based controller for speed control of switched reluctance motor drives," *International Journal of Electrical Power and Energy Systems*, vol. 62, pp.364-373, 2014.

[27] M. H. Vafaie, B. Mirzaeian Dehkordi, P. Moallem, and A. Kiyoumarsi, "A new predictive direct torque control method for improving both steady-state and transient-state operations of the PMSM," *IEEE Transactions on Power Electronics*, vol. 31, no. 5, pp.3738-3753, May 2016.

[28] Y. Sangestani, S. Ziaenejad, A. mehrizi, H. Pairodi-Nabi, and A. Shoulaie, "Estimation of stator resistance in direct torque control synchronous motor drives," *IEEE Transaction on Energy Conversion*, vol. 30, no. 2, pp. 626-634, 2015.

[29] E. Dryabeigi and S. Vaez-Zadeh, "A combined control for fast and smooth performance of IPM motor drives over wide operating conditions," *IEEE Transaction on Energy Conversion*, vol. PP, no.99, pp.1-1, 2018.